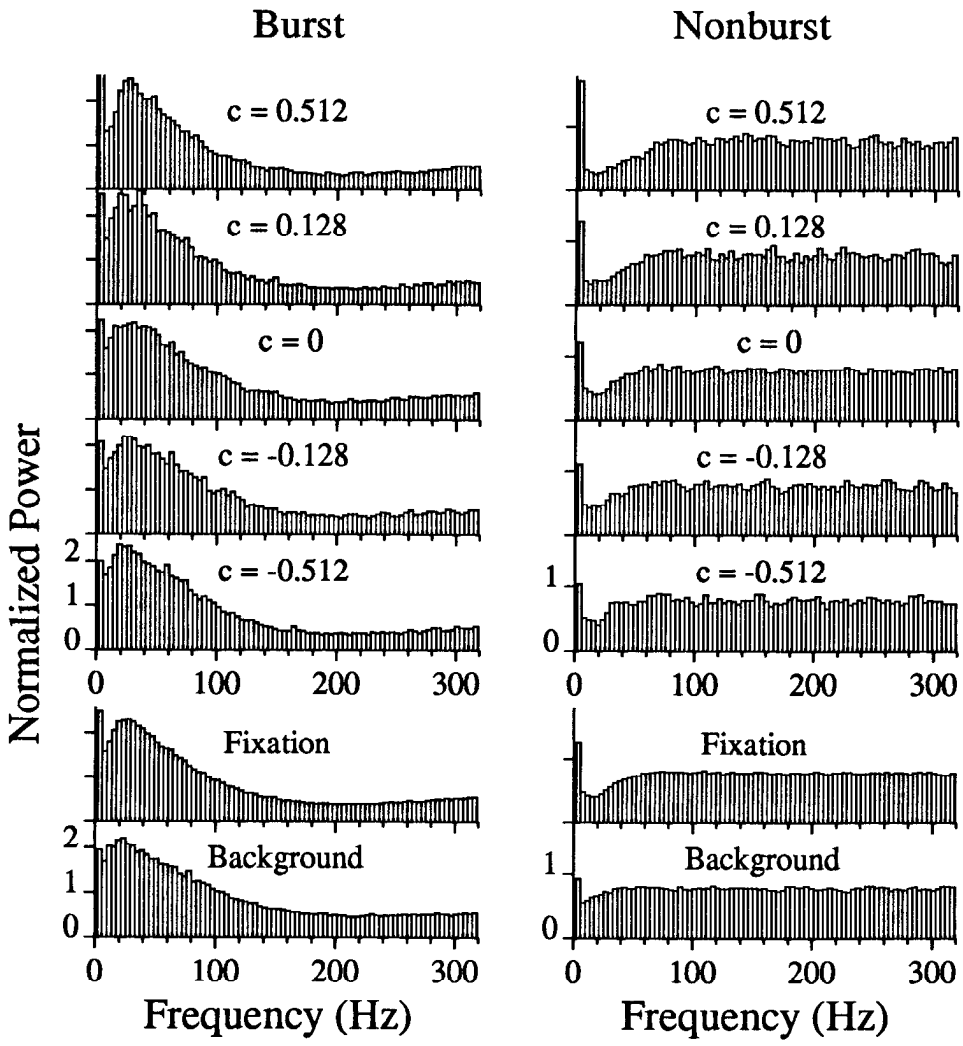

Figure 5. Power spectra, $S'(f)$, are shown for motion coherence values ranging from highly coherent preferred direction motion ($c = 0.512$) to highly coherent null direction motion ($c = -0.512$) for the burst cell (a) and the nonburst (d) cells from Figure 2. Spectra are also shown for background, that is, spontaneous activity, and fixation conditions. The spectra vary little, except that the dip below 20 Hz becomes more prominent when spike rate increases. This can be explained by the potentially greater effect of a refractory period at higher spike rates. These spectra are normalized by spike rate.

pacemaker cell "oscillating" in the 20–60 Hz band, P becomes arbitrarily large as the oscillation becomes increasingly regular.

With P as a measure of the shape of S', we developed a measure of burstiness based on the ISI. Given the well-known distinction between bursting and nonbursting cells based on intracellular current injections in rodent slice preparations (McCormick et al., 1985; Connors and Gutnick, 1990), we attempted to find a metric that would classify all of our cells into two (or more) segregated groups according to the degree of burstiness. For this purpose, we introduce the measure B as the percentage of the ISI histogram in the 1, 2, and 3 msec bins.

The variable B is similar to other proposed measures of burstiness that are based on the proportion of the ISI distribution below a cutoff value (Cattaneo et al., 1981b; Abeles, 1982). We also considered another measure of burstiness, $\tilde{B}$, based on the ratio of the number of intervals in the 2 msec ISI bin to the 5 msec ISI bin. This variable has the potential advantage that it is able to distinguish between a bursting cell with a bimodal ISI histogram and a very fast firing cell that has a unimodal ISI histogram concentrated below about 10 msec. However, $\tilde{B}$ is quite sensitive to fluctuations in the trough between the peaks of a bimodal histogram, and its value is less stable. We will use B as the measure of burstiness here but point out that B and $\tilde{B}$ tend to be highly correlated, at least for our database.

Figure 3 shows the frequency distribution for these three statistical measures for all cells averaged over all stimulus conditions. We interpret the histogram for P to represent a unimodal distribution. The dip at unity is an artifact of our classification system because P is based on regions of the power spectrum that are chosen for maximizing the peak-to-trough ratio or minimizing the trough-to-baseline ratio for burst and nonburst cells, respectively. The long left tail of the distribution for B shows that many cells have less than 1% of their intervals shorter than or equal to 3 msec, such as cell *d* of Figure 2. The distribution for $\tilde{B}$ is spread over many orders of magnitude and shows a hint of bimodality. Overall, however, it is difficult to segment the data into two classes based on these histograms, since many burst and nonburst cells fall in overlapping regions in the histograms for B and $\tilde{B}$. We stress, therefore, that the burst and nonburst classifications are primarily tools for defining two ends of what appears to be a continuum.

For burst cells, P changes relatively little with stimulus condition and appears to reflect primarily an intrinsic property of these cells in an alert and trained monkey. As we show next, in such cells P is highly correlated with B. For nonburst cells, B often changes systematically with spike rate and is therefore not as revealing about intrinsic properties.

The close connection between bursting and the shape of the